Monatshefte für Chemie 120, 941 – 954 (1989)

Monatshefte für Chemie
Chemical Monthly

An Angular Overlap Model Treatment of Mixed Valence Pt(II) – Pt(IV) Haloamine Chain Complexes

Hans-Herbert Schmidtke[1,*] and **Michael A. Atanasov**[2]

[1] Institut für Theoretische Chemie, Universität Düsseldorf, D-4000 Düsseldorf 1, Federal Republic of Germany
[2] Institute of General and Inorganic Chemistry, Bulgarian Academy of Science, Sofia, Bulgaria

Summary. A recently proposed extension of the angular overlap model (AOM) is applied to the linear chain compounds $[Pt^{II}(AA)_2 \cdot Pt^{IV}X_2(AA)_2]^{4+}_{\infty}$ with X = Cl, Br, I; AA = ethylenediamine, 1,2- and 1,3-diaminopropane, and to Wolffram's red and Reihlen's green salt. The energy band structures are calculated from AOM parameters which are derived from d – d spectra of isolated Pt(II) and Pt(IV) complexes reported in the literature. Assignments of absorption edges and other peaks in the crystal spectra as well as spectral shifts due to changes in the geometric structure are discussed. Since the AOM energy expressions are given in analytical form, the procedure supplies various advantages over the extended Hückel theory which currently has been adapted for treating chain structures.

Keywords. Electronic band structures; Linear Pt chain compounds; Crystalline absorption spectra.

Behandlung von gemischt-wertigen Pt(II) – Pt(IV)-Ketten-Komplexverbindungen mit dem „Angular Overlap"-Modell

Zusammenfassung. Eine kürzlich vorgeschlagene Erweiterung des „Angular Overlap"-Modells (AOM) wird auf die linearen Kettenverbindungen $[Pt^{II}(AA)_2 \cdot Pt^{IV}X_2(AA)_2]^{4+}_{\infty}$ mit X = Cl, Br, I; AA = Ethylendiamin, 1,2- und 1,3-Diaminopropan sowie auf Wolffframs Rot- und Reihlens Grün-Salz angewandt. Die Energiebänder werden von AOM-Parametern berechnet, die aus d – d-Spektren isolierter Pt(II)- und Pt(IV)-Komplexe gewonnen wurden, welche in der Literatur zu finden sind. Diskutiert werden Zuordnungen zu Absorptionskanten und anderen Maxima in den Kristallspektren ebenso wie spektrale Verschiebungen aufgrund von Änderungen in der geometrischen Struktur. Da die AOM-Energieausdrücke in analytischer Form vorliegen, hat dieses Verfahren diverse Vorteile im Vergleich zur „Extended Hückel"-Theorie, die kürzlich ebenfalls so erweitert wurde, daß damit Kettenstrukturen behandelt werden können.

Introduction

Recently the angular overlap model (AOM) applicable for investigating electronic structures of transition metal complexes has been extended for treating linear chain compounds in the tight binding scheme by introducing translational symmetry restrictions [1]. This method has several advantages over the extended Hückel theory (EHT) which by proper modification also has been applied for calculating electronic band structures [2]. The AOM uses a much smaller number of model parameters which is about half of that in EHT, and band energy equations can be expressed in general by analytical formulas depending on the wave vector k. Since

the AOM has turned out to be quite successful for interpreting electronic spectra as well as magnetic and structural properties of transition metal complexes, it is felt that this model could also be used for demonstrating the close relations evident between the spectral properties and the geometric structure of infinite chain compounds. Most suitable for this purpose would be an investigation of mixed valence compounds exhibiting pronounced spectroscopic absorptions due to very strong charge transfer transitions in the visible region.

Characteristic representatives for this class of compounds are Pt(II)–Pt(IV) complexes of the type $[M^{II}(AA)_2 \cdot M^{IV}X_2(AA)_2]^{4+}$ with bridging atoms X = Cl, Br and I and amine ligands AA = ethylenediamine (*en*), 1,2-diaminopropane (*pn*), 1,3-diaminopropane (*tn*) or the Wolffram's red salt $[Pt(NH_2C_2H_5)_4 \cdot PtCl_2(NH_2C_2H_5)_4]Cl_4 \cdot 4H_2O$ (*WR*) and the corresponding bromine compound, i.e. Reihlen's green salt (*RG*) [3, 4]. All of their crystal structures are known [4–6], they form singly bridged chains ($\cdots$Pt(II)$\cdots X$-Pt(IV)-$X\cdots$) along one of the crystallographic axes with alternating units of square planar PtA_4^{2+} and hexacoordinated $PtX_2A_4^{2+}$ chromophoric units, the Pt(IV)-X bond lengths, in general, being smaller than Pt(II)$\cdots X$ atomic distance. All APtX bond angles are close to 90°. The structural data and physical properties of these systems allow an ordering into class II mixed valence compounds according to the classification of Robin and Day [7], i.e. they are diamagnetic [8] and exhibit solid state spectra characteristic for the isolated constituent complex units, but contain in addition strong absorptions assigned to intervalence charge transfer transitions [3, 9, 10]. Increasing the temperature or applying high pressure leads to significant changes of physical properties such as low energy shifts of the charge transfer absorptions [11, 12] and a reversible increase of electric conductivity by a factor of 10^9 at 140 kbar [13]. Due to X-ray diffraction studies carried out also at different pressure, these property changes can be correlated to varying structural parameters. Since detailed experimental results on absorption, emission, reflectance and excitation spectra as well resonance raman data are available for these compounds [9–14], they represent appropriate examples for testing the extended AOM on these systems, demonstrating the relations pertinent to optical or other physical properties and the structure of these transition group complexes. Moreover, for Pt compounds the d − d spectra of various mononuclear are known [15–19] from which ligand field AOM parameters are derived serving as useful reference values for the present chain compounds.

The only theoretical treatment of this type of chain compounds was carried out on a model compound as $[Pt(NH_3)_4 \cdot Pt(NH_3)_4X_2]^{4+}$ applying EHT [20] which, although the non-diagonal elements of the orbital energy matrix are approximated by a modified Wolfberg-Helmholz formula [21], leads to a large number of atomic parameters (eight for the diagonal elements and ten for exponents in the Slater-type orbitals for calculating overlap integrals). This calculation has considered a high symmetric chain of $Pt^{III}A_4X$ units, as the bridging halide ions are located on the midpoints between the metal ions, and showed how a band gap is opened stabilizing the system on geometry distortion which leads to a Pt-X bond alternation.

In the present paper we show that energy bands of the electronic level schemes can be obtained from the AOM at much smaller expense of computation than from EHT furnishing similar results, the AOM parameters being derived from smaller molecular units available from isolated mononuclear complexes. The results will be used for explaining the electronic spectra of the title linear chain compounds.

Structural Data and Electronic Spectra

A collection of crystal data for the present chain compounds is supplied by Keller [4] and references given in his review article. Important bond lengths for an AOM treatment are those for *M-X* and *M*-N with *M* = Pt(II) and Pt(IV), since the size of the model parameters and the phenotype of the optical spectra are primarily determined by the metal-ligand bond moiety. In virtual all cases the *M-X* bond lengths for Pt(II) are significantly larger than for Pt(IV) except for the bromine compound of *en* and *pn* where the halogene atom is located almost on the center of the linear Pt-Br-Pt group of atoms [4], the Pt-Br bond distances of 271 pm for Pt^{IV}-Br and 276 pm for Pt^{II}-Br in the *en* compound comparing with 244.5 pm in K_2PtBr_4 [22]. The structural parameters of the corresponding chloro-*en* (*en*Cl) compound [4] are 231.8 for Pt ^{IV}-Cl and 308.5 pm for Pt ^{II}-Cl in the perchlorate salt and in the isolated species 232 pm for K_2PtCl_6 [23] and 231.6 pm for K_2PtCl_4 [24]. Of similar importance are Pt-N bond lengths which in the chain compounds vary from 197 to 212 pm, the Pt^{IV}-N distances in general being a few picometer smaller than for Pt^{II}-N. These numbers compare, e.g., to 206–209 pm in *tr*$[Pten_2X_2]^{2+}$ (*X* = Cl, I) [25] and 205–206 in $[Pt(tn)_2]^{2+}$ [26]. It should be noted, however, that structural data for some of the compounds have large error limits due to severe twinning of the crystals or a lack of three-dimensional order because of occasional shifts of one chain molecule to another, sometimes accompanied by stacking faults.

Table 1. Absorption features from polarized single crystal spectra (π: $\vec{E} \parallel z$ and σ: $\vec{E} \perp z$) according to Ref. [11] listing absorption edges *P* and band maxima *Q*, α, β in μm^{-1}

Compound	*T*(K)	Polarization	*P*	*Q*	α	β
	RT[a]	π	1.75	2.2[b]	2.87	
		σ	(b)	–	2.91	
*en*Cl						
	2	π	1.91	2.20[b]	2.97	
		σ	(b)	2.21	3.00	
	RT	π	0.775	2.06	2.53	
		σ	–	2.08	2.54	3.49
*en*I						
	2	π	0.845	2.04	2.52	
		σ	~0.8[c]	2.05	2.54	3.48
	RT	π	1.62	(b)		
		σ	(b)	(b)	2.53	
WR[d]						
	2	π	1.79	2.12[c]		
		σ	1.6[c]	2.12		

[a] Room temperature
[b] Shoulder
[c] Weak absorption
[d] Peaks in agreement with Ref. [14]

Table 2. Band maxima υ in μm^{-1} from diffuse reflectance spectra and bond distances in pm from Ref. [3] and [4] and references therein

Compound	Property[a]	Counter Ion	
		ClO_4^-	BF_4^-
*en*Cl	υ	2.273	2.00
	R (R')	231.8 (308.5)	
	R^0 ($R^{0'}$)	202 (207)	
*tn*Cl	υ	2.296	2.062
	R (R')		229.9 (309.6)
	R^0 ($R^{0'}$)		207 (207)
*pn*Cl	υ	2.353	2.151
	R (R')	231 (320)	
	R^0 ($R^{0'}$)	200; 211 (200; 211)[b]	
*en*Br	υ	1.515	1.408
	R (R')	271 (276)	
tn(Br)	υ	1.653	1.408
	R (R')	254.6 (295.5)	254.1 (292.1)
	R^0 ($R^{0'}$)	204 (208)	212 (209)
pn(Br)	υ	1.77	1.587
	R (R')	267 (267)[c]	
*en*I	υ	1.23	
*tn*I	υ	1.23	1.23
*pn*I	υ	1.23	1.23

[a] Metal-halogen R and metal-nitrogen R^0 bond distances (see text)
[b] Asymmetric coordination
[c] Bromide as counter ion

In Tables 1 and 2 spectroscopic data available from polarized absorption spectra and from diffuse reflectance for the presently interesting compounds are listed as they are reported in the literature. The reflectance spectra are dominated by a broad absorption peak (Table 2) due to a d_{z2} electron transition from Pt(II) to Pt(IV) [27, 28] which corresponds in the single crystal spectra to a pronounced absorption edge P (Table 1) polarized along the chain direction [11, 12, 14]. This assignment agrees with resonance Raman results obtained from some of the chain compounds which exhibit at energy close to the absorption edge a long progression in the symmetric Pt-X-Pt stretching mode [12, 14, 27]. Based on the EHT calculations [20] the band Q predominantly polarized perpendicular to z has been assigned to charge transfer transitions from d_{xz}, d_{yz} of primarily Pt(II) to d_{z2} of Pt(IV) [11]. The peaks α and β towards higher energy, which are also observed in aqueous solution where decomposition into the complex constituents can be assumed, are according to the same authors [11] due to local transitions. In the chain

compounds charge transfer transitions between d-orbitals of Pt(II) and Pt(IV) should also contribute to the intensity of the β-peak [11]. Weaker band features lower or somewhat higher in energy of the absorption edge which are not listed in Tables 1 and 2 are reported to correspond to excitons, localized impurity states or probably plasmons [11, 12, 28]. The occurrence of excitons has been discussed in detail, yet the actual mechanism of their origin has not been clarified so far [11, 12]. Since Raman scattering does not resonate at energies lower than the absorption edge (also the excitation spectrum and first-order Raman cross sections yield negligibly small resonance features in this region [12]) we safely can assume that no other transitions than those occurring between the d-electron band scheme have to be considered in the present systems. On temperature increase, the absorption edge P is observed to decrease in energy at the same time gaining some more intensity. These changes as well as the variation with pressure [13] will be discussed later (vide infra).

Theoretical Results

Electronic Structure of Chain Molecules Derived from the AOM

The energy band scheme due to crystal orbitals from the d-orbital subset of the singly bridged $[Pt(N)_4 \cdots XPt(N)_4X \cdots]^{4+}$ chain chromophore is obtained from a tight-binding approximation applied on the basis of the AOM [1]. For a linear arrangement of the metal-ligand bonds the secular problem is separated into non-interacting σ- and π-bond equations due to symmetry reasons (cf. Fig. 1). Using a perturbation formalism, the one-electron secular problem is reduced into the subspace of metal d-orbitals, the energy matrix elements of which are denoted by U_{ij} with indices referring to orbitals on metal centers i and j. The d-orbital perturbation matrix for a chain of two metals in the unit cell of length a depending on the wave vector k is

$$\begin{matrix} & d_\lambda{}^1 & d_\lambda{}^2 \\ \begin{matrix} d_\lambda{}^1 \\ d_\lambda{}^2 \end{matrix} & \begin{pmatrix} U_{d_\lambda{}^1 d_\lambda{}^1} & 2\cos(ka/2)\, U_{d_\lambda{}^1 d_\lambda{}^2} \\ 2\cos(ka/2)\, U_{d_\lambda{}^1 d_\lambda{}^2} & U_{d_\lambda{}^2 d_\lambda{}^2} \end{pmatrix}, \end{matrix} \tag{1}$$

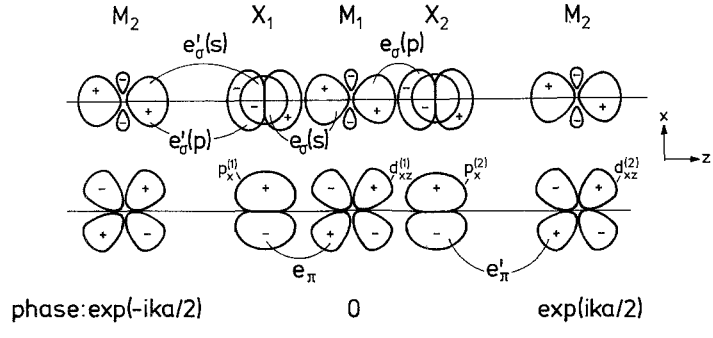

Fig. 1. Definition of valence orbital sets for σ- and π- antibonding interactions

where λ denotes the type of bonding, i.e. $\lambda = \sigma$ through d_{z^2}-, $\lambda = \pi$ through d_{xz}, d_{yz}- and $\lambda = \delta$ through d_{xy}, $d_{x^2-y^2}$-orbitals at centers 1 and 2. Parametrization in the AOM furnishes in the case of the σ-bonding part

$$\begin{aligned} &\text{Pt(IV):} \quad U_{d_\sigma 1\, d_\sigma 1} = e_\sigma{}^0 + 2e_\sigma(s) + 2e_\sigma(p) = e_\sigma{}^0 + 2e_\sigma, \\ &\text{Pt(II):} \quad U_{d_\sigma 2\, d_\sigma 2} = e_\sigma{}^{0'} + 2e_\sigma'(s) + 2e_\sigma'(p) = e_\sigma{}^{0'} + 2e_\sigma', \end{aligned} \tag{2}$$

where different AOM parameters for the short Pt(IV) (unprimed) and the long Pt(II) (primed) metal-ligand bonds of M-X (e_σ) and M-N ($e_\sigma{}^0$) interaction are introduced. For the two-center matrix element we obtain [1]

$$U_{d_\sigma 1\, d_\sigma 2} = [e_\sigma(s)\, e_\sigma'(s)]^{1/2} - [e_\sigma(p)\, e_\sigma'(p)]^{1/2}. \tag{3}$$

The eigenvalues of Eq. (1) are

$$\begin{aligned} E_k^{\mathrm{II,IV}}(d_{z^2}) = \frac{1}{2}(e_\sigma{}^0 + e_\sigma{}^{0'}) + e_\sigma + e_\sigma' \mp \frac{1}{2}\{(\Delta e_\sigma{}^0 + 2\Delta e_\sigma)^2 \\ + 16\cos^2(ka/2)\,[(e_\sigma(s)\, e_\sigma'(s))^{1/2} - (e_\sigma(p)\, e_\sigma'(p))^{1/2}]^2\}^{1/2} \end{aligned} \tag{4}$$

with

$$\Delta e_\sigma{}^0 = e_\sigma{}^0 - e_\sigma{}^{0'} \qquad \text{and} \qquad \Delta e_\sigma = e_\sigma - e_\sigma', \tag{5}$$

reflecting possible alternations in respective metal-ligand bonds. The notation for the roots E_k^{II} and E_k^{IV} refers to Pt(II) and Pt(IV) d-orbital components since, due to $e_\sigma' < e_\sigma$, eigenfunctions belonging to E_k^{II} have larger contributions from d-orbitals of Pt(II) and functions to E_k^{IV} larger orbital contributions from Pt(IV) (vide infra). In the case of equal Pt-N and Pt-Cl bond distances, Eq. (4) simplifies to

$$E_k^{\mathrm{II,IV}}(d_{z^2}) = e_\sigma{}^0 + 2e_\sigma \mp 2\cos(ka/2)\,[e_\sigma(p) - e_\sigma(s)], \tag{6}$$

which does not supply a band gap at $k = \pi/a$ since the last term in Eq. (6) vanishes at this value of k.

For alternating bonds the band gap arising at $k = \pi/a$ is calculated from Eq. (4),

$$\Delta E_{\pi/a} = E_{\pi/a}^{\mathrm{IV}} - E_{\pi/a}^{\mathrm{II}} = \Delta e_\sigma{}^0 + 2\Delta e_\sigma, \tag{7}$$

which is positive for any e_σ parameter values, i.e. the band originating primarily from Pt(IV) d-orbitals is always higher in energy than the band from Pt(II) orbitals. A larger energy separation is obtained at $k = 0$ as is calculated also from Eq. (4) which yields

$$\begin{aligned} \Delta E_0 &= E_0^{\mathrm{IV}} - E_0^{\mathrm{II}} \\ &= \{(\Delta e_\sigma{}^0 + 2\Delta e_\sigma)^2 + 16\,[(e_\sigma(s)\, e_\sigma'(s))^{1/2} - (e_\sigma(p)\, e_\sigma'(p))^{1/2}]^2\}^{1/2}. \end{aligned} \tag{8}$$

The π-bonding matrix elements of Eq. (1) referring to π-orbitals in the x- and y-plane aligned at maximal overlap (cf. Fig. 1) are

$$\begin{aligned} U_{d_\pi 1\, d_\pi 1} &= 2e_\pi{}^0 + 2e_\pi, \\ U_{d_\pi 2\, d_\pi 2} &= 2e_\pi{}^{0'} + 2e_\pi', \\ U_{d_\pi 1\, d_\pi 2} &= -(e_\pi e_\pi')^{1/2}. \end{aligned} \tag{9}$$

Solution of the secular problem leads to the eigenvalues

$$E_k^{\mathrm{II,IV}}(d_{xz}, d_{yz}) = e_\pi{}^0 + e_\pi{}^{0'} + e_\pi + e_\pi{}' \mp [(\Delta e_\pi{}^0 + \Delta e_\pi)^2 + 4\cos^2(ka/2)\, e_\pi e_\pi{}']^{1/2}, \tag{10}$$

which are degenerate for d_{xz} and d_{yz} orbital sets. In case of neglecting δ-bonding ($\lambda = \delta$) the corresponding energy expressions are

$$\begin{aligned} E_k^{\mathrm{IV}}(d_{xy}) &= 4\, e_\pi{}^0, & E_k^{\mathrm{IV}}(d_{x^2-y^2}) &= 3\, e_\pi{}^0, \\ E_k^{\mathrm{II}}(d_{xy}) &= 4\, e_\pi{}^{0'}, & E_k^{\mathrm{II}}(d_{x^2-y^2}) &= 3\, e_\pi{}^{0'}, \end{aligned} \tag{11}$$

which are independent of k.

Parameter Choice

The AOM parameters e_λ used for the present chain compounds shall be derived from parameters which are calculated from the spectra of isolated mononuclear Pt(II) and Pt(IV) complexes of similar composition. The number of parameters can, however, be decreased significantly. First of all, the $e_\pi{}^0$ parameters of Pt-N vanish due to the lack of low-lying amine orbitals of π-symmetry [18]. Moreover, the dependence of AOM parameters on the metal-ligand bond lengths can be used for expressing e_λ parameters belonging to smaller R by $e_\lambda{}'$ parameters of larger R' or vice versa. This is achieved by relating

$$\frac{e_\lambda}{e_\lambda{}'} = \left(\frac{R'}{R}\right)^n \qquad \text{for} \qquad \lambda = \sigma \quad \text{or} \quad \pi, \tag{12}$$

where n is a number between 5 and 7 depending on the model which is used for formulating the R-dependence of the cubic ligand field parameter $10\,Dq = 3\, e_\sigma - 4\, e_\pi$: in the framework of classical ligand field theory [29] we calculate $n = 5$ whilst in a pseudopotential model $n = 7$ has been derived [30]. For a series of Ni(II) amine complexes, e.g., an $n = 4$–5 dependence is obtained from the experiment [31]. With these additional assumptions, the number of model parameters is reduced to only four or five, i.e. $e_\sigma{}^0$, $e_\sigma(s)$, $e_\sigma(p)$, e_π and eventually n.

Actual parameter values for the Pt(IV) amine interaction can be, e.g., derived from the ligand field strength $10\,Dq$ of $[Pten_3]^{4+}$ which is reported [15] to be $4.65\,\mu m^{-1}$, well in agreement with Jørgensen's product formula [32] $10\,Dq = f \cdot g$, yielding for f (NH_3) = 1.25 and g (Pt^{IV}) = $3.6\,\mu m^{-1}$ the ligand field parameter $10\,Dq = 4.5\,\mu m^{-1}$. From $10\,Dq = 3\, e_\sigma{}^0 - 4\, e_\pi{}^0$ with vanishing $e_\pi{}^0$ we obtain $e_\sigma{}^0 = 1.5$ to $1.55\,\mu m^{-1}$. For a square planar Pt(II) ammonia complex on the other hand an $e_\sigma{}^0$ value of $1.33\,\mu m^{-1}$ can be calculated [18]. Since Pt-N bond lengths R^0 in present chain systems vary only about 6% for Pt(II) and Pt(IV), in general a common $e_\sigma{}^0$ parameter may be used.

For Pt-Cl interactions the parameters $e_\sigma = e_\sigma(s) + e_\sigma(p) = 1.24$ and $e_\pi = 0.28\,\mu m^{-1}$ are adopted [18, 19] which apply for the atomic distance $R = 232$ pm as reported [24] for K_2PtCl_4. Due to the smaller d_M-s_L overlap the $e_\sigma(s)$ parameter is about 10% of $e_\sigma(p)$ parameters [1]. From the experiment a partitioning of the e_σ parameter into $e_\sigma(s)$ and $e_\sigma(p)$ cannot be obtained. The inclusion of a further σ_{sd} parameter for considering the intermixing of d and higher

metal s orbitals which is important for square planar complexes [10, 18] does not contribute significantly to the electronic structure of the present chain compounds since the polar coordination sites in z-direction are occupied by halogen ligands at distance R'. For Pt-Br the parameter values become $e_\sigma = 1.09$ and $e_\pi = 0.22\,\mu m^{-1}$ which are valid for 244.5 pm as derived from K_2PtBr_4 [22]. These parameters refer to bond lengths which are close to the Pt^{IV}-X bond distances in Pt(II)-Pt(IV) chain molecules, therefore they can be used as starting sets for parametrizing the short Pt-X bond interactions in the present calculations. Corresponding parameters for the long Pt-X bonds are then obtained from Eq. (12).

Parameters for Pt-I bonds are lacking since $d-d$ transitions are for the most part covered by large ligand to metal charge transfer absorptions preventing the determination of AOM parameters from the experiment. They may be, however, extrapolated from Cr^{III}-X parameters [33, 34] by relating corresponding metal-halogen parameters in the series X = Cl, Br, I. This procedure yields $e_\sigma = 0.97$ and $e_\pi = 0.19\,\mu m^{-1}$ for reasonable Pt-I estimates.

Discussion

Some energy band schemes computed from AOM parameters suitable for Cl-bridged chain compounds are presented in Fig. 2. In calculation (a) the two components $e_\sigma(s)$ and $e_\sigma(p)$ of the e_σ-parameter are considered separately. The band positions do not differ very much from the calculation (b) where the σ interaction is combined into a single e_σ-parameter. Only the d_{z^2} band widths are narrower in calculation (a) since bonds are more localized if s- and p-orbitals are allowed to hybridize which decreases at the same time the overlap between atomic orbitals of different units cells. For equal Pt-X atomic distances (non-alternating bonds) the band system depicted in Fig. 2c is obtained where a set of parameters averaged over e_λ and e_λ' is used. The parameters applying to the longer Pt-X bond distances in each case are calculated from Eq. (12) for $n = 5$.

Also the density of states is plotted on the figures as calculated by means of the histogram method [35] using the formula

$$D(E_i) = \sum_n \sum_k \delta^{\Delta E}[E_i - E_n(k)], \tag{13}$$

where the summation n extends of the energy bands and k over a number of selected points in the Brillouin zone. The Kronecker symbol is

$$\delta^{\Delta E}[E_i - E_n(k)] = \begin{cases} 1, & \text{if } |E_i - E_n(k)| \leqq \Delta E/2, \\ 0, & \text{otherwise,} \end{cases} \tag{14}$$

when the interval $\Delta E = E_{i+1} - E_i$ is chosen to be small compared to the width of the band.

The energy gap calculated from Eq. (7) with parameters given in the preceding section is $\Delta E = 1.88$–$2.14\,\mu m^{-1}$ for the chloro-*en* chain (*en*Cl) compound and 0.89–$1.12\,\mu m^{-1}$ for *en*I depending, respectively, on the power $n = 5$ or 7 used in Eq. (12). Comparison with the absorption edge measured at $1.91\,\mu m^{-1}$ for *en*Cl and $0.847\,\mu m^{-1}$ for *en*I (i.e. the low temperature results of Table 1) suggests that an $n = 5$ dependence of e_λ parameters would be the more appropriate choice in Eq.

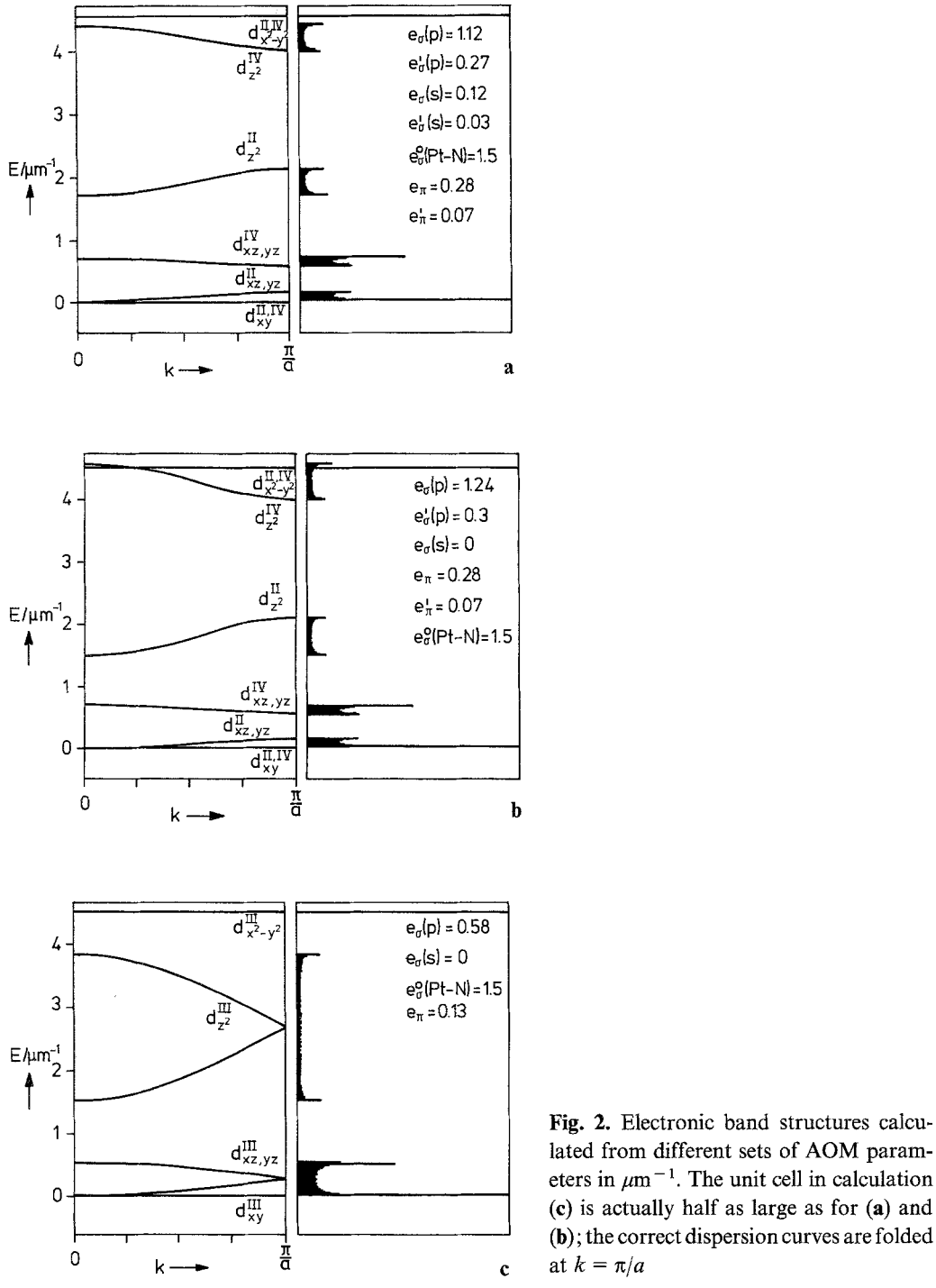

Fig. 2. Electronic band structures calculated from different sets of AOM parameters in μm^{-1}. The unit cell in calculation (**c**) is actually half as large as for (**a**) and (**b**); the correct dispersion curves are folded at $k = \pi/a$

(12) which is in accordance with the predictions of conventional ligand field theory [29]. The spectrum of the *en*Cl compound moreover allows for determining the AOM parameters of the Pt^{IV}-Cl interaction which are unknown until now: from Eq. (7) and the R-dependence of e_σ(Pt-Cl) supplied by Eq. (12) using $n = 5$, we obtain $e_\sigma(Pt^{IV}\text{-Cl}) = 1.15\,\mu m^{-1}$ and, with $10\,Dq = 2.84\,\mu m^{-1}$, $e_\pi(Pt^{IV}\text{-Cl}) =$

$= 0.14\,\mu m^{-1}$ (for $R = 232\,pm$) which is smaller than $e_\pi(Pt^{II}\text{-}Cl)$ obtained from $PtCl_4^{2-}$ (see above). For the bromium chain compound RG we calculate with the Pt-Br parameters $e_\sigma = 1.09\,\mu m^{-1}$ for $R = 246\,pm$, $R' = 312\,pm$[4] and $n = 5$ an energy gap of $\Delta E = 1.46\,\mu m^{-1}$ which compares quite well with the resonance Raman result of $1.59\,\mu m^{-1}$ reported by Clark and Turtle [36].

Reasonable assignments of the *en*Cl spectrum in Table 1 on the basis of the calculated band scheme, which are in accordance with C_{4v} selection rules of wave vector k and measured polarizations, are

$$
\begin{array}{lll}
P & d_{z^2}^{II} \rightarrow d_{z^2}^{IV} & \text{for } k = \pi/a,\ a_1 \rightarrow a_1,\ z(\parallel)\text{ polarized,} \\
Q & d_{z^2}^{II} \rightarrow d_{x^2-y^2}^{II,IV} & \text{for } k = \pi/a,\ a_1 \rightarrow b_1,\ \text{electronically forbidden,} \\
\alpha & \left\{ \begin{array}{l} d_{xz}^{IV}, d_{yz}^{IV} \rightarrow d_{z^2}^{IV} \\ d_{z^2}^{II} \rightarrow d_{z^2}^{IV} \end{array} \right. & \begin{array}{l} \text{for } k = \pi/a,\ e \rightarrow a_1,\ x,y(\perp)\text{ polarized,} \\ \text{for } k = 0,\ a_1 \rightarrow a_1,\ z(\parallel)\text{ polarized.} \end{array}
\end{array}
$$

Accordingly, the weak absorption Q observed in either polarization is only vibronically allowed obtaining in *en*I higher intensity because of large vibronic coupling to low lying charge transfer states. In the iodine complex both the strong absorptions α and β are due to charge transfer transitions. In both compounds α and β are localized transitions occurring at the PtN_4X_2 chromophoric centers, their positions and assignments agreeing well with the spectra which are obtained for isolated $[Pten_2X_2]^{2+}$ [16]. However, when comparing experimental absorption maxima with crystal orbital energy differences obtained from the calculation, one should keep in mind that transferring electrons from a localized to a more delocalized orbital or vice versa, e.g. $d_{z^2} \rightarrow d_{x^2-y^2}$, will also change the electron repulsion which sometimes supplies quite drastic contributions. Therefore crystal orbital energy differences, in general, cannot predict actual positions of absorption peaks very accurately. The proposed assignments are in part also in variance with earlier suggestions [11, 14].

The *WR* absorption spectrum is shifted compared to the *en*Cl spectrum to lower wavelengths (cf. Table 1). An explanation on the basis of geometry changes is difficult to propose since the structural data of WR are not very accurate [5]. Apparently, the AOM parameters of *WR* are somewhat different to those of *en*Cl; in particular the large shift of the α peak from 2.91(*en*Cl) to $2.53\,\mu m^{-1}$ (*WR*) could be explained by increased π-antibonding effects in d_{xz}^{IV} and d_{yz}^{IV} orbitals leading to a certain destabilization of corresponding bands for the *WR* compound by virtue of larger e_π and probably also finite e_π^0 parameters in Eq. (10).

For an investigation of the d-electron density distribution on Pt(II) and Pt(IV) metal centers, we consider the wave functions using the procedure as outlined earlier [1]. For convenience only that parts of the functions which refer to a single unit cell is given, and we set in the σ-type orbitals of d_{z^2}-bands $e_\sigma^0 = e_\sigma^{0'}$ and $e_\sigma(s) = 0$. With these assumptions we calculate the d_{z^2}-functions (not normalized) for $k = 0$:

$$
\begin{aligned}
E_{k=0}^{II}(d_{z^2}) &= e_\sigma^0, & \psi_{k=0}^{II} &= (e_\sigma + e_\sigma')^{-1/2}(e_\sigma'^{1/2} d_{z^2}^1 + e_\sigma^{1/2} d_{z^2}^2), \\
E_{k=0}^{IV}(d_{z^2}) &= e_\sigma^0 + 2(e_\sigma + e_\sigma'), & \psi_{k=0}^{IV} &= (e_\sigma + e_\sigma')^{-1/2}(e_\sigma^{1/2} d_{z^2}^1 + e_\sigma'^{1/2} d_{z^2}^2) \\
& & & \quad -[(e_\sigma + e_\sigma')/(H_M^0 - H_p^0)]^{1/2}(p_z^1 - p_z^2).
\end{aligned}
\tag{15}
$$

Also contributions due to orbitals on the amine ligands are neglected since they do not participate in the energy band formation. Since e_σ' refers to the longer Pt^{II}-X and e_σ to the shorter Pt^{IV}-X bonds, from Eq. (12) we have $e_\sigma' < e_\sigma$. Therefore, the crystal orbitals of the lower band d^{II}_{z2} are dominated by d^2_{z2} (Pt^{II}) and those of the higher band d^{II}_{z2} by d^1_{z2} (Pt^{IV}) atomic orbitals, which means that $d^{II}_{z2} \rightarrow d^{IV}_{z2}$ transitions transfer d_{z2} electrons mainly localized on Pt(II) to Pt(IV), the orbitals of the latter extending partially also over halogen ligands. For bond distances and e_σ bond parameters as used above, the d_{z2} electron density on Pt(IV) is calculated 0.19 for the *en*Cl chain compound, 0.48 for *en*Br and 0.35 for *en*I. The corresponding EHT result [20] of only 0.03 obtained for *en*Cl supplies a *d*-electron distribution which probably is too much localized on Pt(II). In the *en*Br compound, where the Br atoms are placed almost midway between the Pt ions, the *d*-electrons are almost completely delocalized over the metal centers leading to a symmetric $d^7 + d^7$ configuration which proposes a structural formula containing Pt^{III}-Br-Pt^{III} atomic groups for this chain compound. A comparison of band energies of systems with and without bond alternation [calculation (b) and (c) of Fig. 2] shows that parallel to the formation of a band gap the total energy is decreased for an electron configuration filling the bands up to d^{II}_{z2}. The system therefore is more stabilized due to the operation of a Peierls distortion favoring low symmetry structures and mixed valence compounds.

The crystal orbitals at the zone boundary $k = \pi/a$ where the band gap between the valence and the conduction band is located are

$$E^{II}_{k=\pi/a}(d_{z^2}) = e_\sigma{}^0 + 2\,e_\sigma', \quad \psi^{II}_{k=\pi/a} = d^2_{z2} - [e_\sigma'/(H_M{}^0 - H_p{}^0)]^{1/2}(p^2_z + p^1_z),$$
$$E^{IV}_{k=\pi/a}(d_{z^2}) = e_\sigma{}^0 + 2\,e_\sigma, \quad \psi^{IV}_{k=\pi/a} = d^1_{z2} + [e_\sigma/(H_M{}^0 - H_p{}^0)]^{1/2}(p^2_z + p^1_z). \qquad (16)$$

The orbitals of Eq. (15) and Eq. (16) are depicted in Fig. 3 illustrating the degree of delocalization from the weight of atomic orbitals inherent in the crystal orbitals.

The AOM results can also explain the low frequency shift and intensity increase of the absorption band elge observed at higher temperature [11] (cf. Table 1) or pressure [13]. Measurements carried out on *WR* show, e.g., a 1.4 kK change of the charge transfer band to lower wave numbers if a pressure of 30 kbar is applied. Shifts to lower energy may be explained from the band gap formula Eq. (7) if the compression is supposed acting in the *z*-direction along the molecular chain $M \cdots X$-M-X. Since the applied force K in this direction is $K = k \cdot \Delta R = k' \cdot \Delta R'$ (assuming harmonic force fields) where the force constant k of the shorter M-X bond is larger than k' of the longer $M \cdots X$ bond, we obtain a more important decrease $\Delta R'$ for the longer bond length than for ΔR of the shorter. With these changes of atomic distances the AOM parameters e_σ and e_σ' become more equal reducing Δe_σ in the band gap formula of Eq. (7). The higher electric conductivity observed when applying pressure on these compounds has been explained by a phonon-assisted electron transfer mechanism between partially localized states [37]. On the basis of AOM results it can be reasoned that as the halide ion moves by vibrational excitation on an average position from Pt(IV) more closely towards Pt(II), the energy gap is decreased in the same way as is the case when applying pressure. The decrease of Δe_σ lowers the barrier for electron transfer processes leading to increased occupancies of the conduction band. In the same way the temperature dependence of the absorption spectra can be understood: a change of only 5 pm to smaller

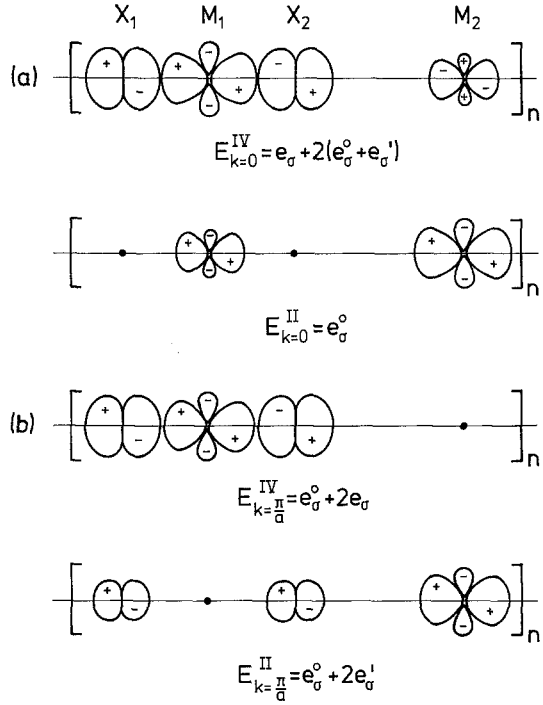

Fig. 3. Atomic orbital contributions to σ-crystal orbitals for (**a**) $k = 0$ and (**b**) $k = \pi/a$. Orbitals on amine ligands are omitted for clarity

(Pt^{II}) and larger (Pt^{IV}) Pt-X separations when increasing the temperature lowers the band gap energy by 0.11 μm^{-1} if Eq. (12) with $n = 5$ is used for the R-dependence of the parameters. This can be compared with a shift of about 0.16 μm^{-1} observed for a temperature change from liquid helium to room temperature in *en*Cl (cf. Table 1).

Similarly, intensity changes may be explained by transition moments M_z which are calculated from the wave function Eq. (16) at the zone boundary. For electric dipole transitions we get if only neighboring atoms are considered

$$M_z \sim (\psi^{II} \,|\, ez \,|\, \psi^{IV}) = (d^2_{z^2} \,|\, ez \,|\, p^2_z - p^1_z)\, K - (p^2_z + p^1_z \,|\, ez \,|\, d^1_{z^2})\, K', \tag{17}$$

with $K = [e_\sigma/(H_M{}^0 - H_p{}^0)]^{1/2}$ and K' calculated from e_σ'. Since the first term vanishes by symmetry reason, M_z becomes

$$M_z \sim -2K'(p^2_z \,|\, ez \,|\, d^1_{z^2}), \tag{18}$$

which increases when lowering the Pt-X distances at higher pressure or temperature due to corresponding changes of e_σ' in K' and, less pronounced, of the transition moment integral $(p^2_z \,|\, ez \,|\, d^1_{z^2})$ which is negative by definition of the wave functions chosen (cf. Fig. 1).

The reflectance spectra [3] (see Table 2) exhibit at long wave lengths pronounced maxima which correspond to the absorption edges P measured in the polarized single crystal spectra. They are, however, shifted throughout to higher energy by about 0.5 μm^{-1}. A discussion of the observed spectroscopical trends in the compound series *en*Cl, *en*Br, *en*I or *en*Cl, *tn*Cl, *pn*Cl etc. cannot be carried out in the same way as above since structural data are missing for most of these compounds.

Although some of the changes seem to be obvious, e.g., the low energy shift with heavier halogen ligands observed in either series of amine compounds is apparent from lower ligand field parameters, there are other relations which need further explanations. There is, for instance, the relatively strong shift of the intervalence band position when changing the counter ion. In the case of the *tn*Br compound, for which structural data of perchlorate and tetrafluoroborate salts are available, the band shift from 1.653 to 1.408 μm^{-1} (cf. Table 2) can be explained by the Pt-N and Pt-Br interatomic distances which are significantly affected by the counter ion. A calculation of the band gap energy Eq. (7), carried out with the AOM parameters e_σ (Pt-N) = 1.43 μm^{-1} for R = 206 pm obtained from an estimation for *tn* on the basis of the spectrochemical series [38] and e_σ (Pt-Br) = 1.09 μm^{-1} for R = 244.5 pm as derived from K_2PtBr_4 [22] and using the structural data of Table 2 in Eq. (12), yields ΔE = 1.08 μm^{-1} for *tn*Br · ClO_4 and 0.81 μm^{-1} for *tn*Br · BF_4. At least the difference of 0.27 μm^{-1} compares well with the band maximum shift of 0.245 μm^{-1} observed for these compounds. Absolute values also agree if the 0.5 μm^{-1} peak change is considered which is measured in the reflectance spectra.

Quite similar relations reported for corresponding Pd(II)–Pt(IV) and Pd(II)–Pd(IV) chain compounds [3] can be explained from the extended AOM as well; however, this would be outside the scope of the present article.

Conclusions

The electronic properties of mixed valence Pt(II)–Pt(IV) chain compounds can be discussed on the basis of the AOM suitably modified for treating extended molecular structures. Absorption edges due to intervalence transitions and other absorption peaks in the crystal spectra are assigned to calculated energy bands using AOM parameters which are derived from isolated mononuclear complexes of Pt(II) and Pt(IV). Relations connecting spectroscopic shifts with geometric distortions of chain molecules, e.g., caused by pressure or temperature changes, can easily be explained from parameter dependences on interatomic distances. The model could appropriately be extended to more complicated systems containing two- or three-dimensional networks.

Acknowledgments

The authors are grateful to the Deutsche Forschungsgemeinschaft, Bonn-Bad Godesberg, for supplying a grant out of the program for promoting scientific work between Bulgaria and the Federal Republic of Germany.

References

[1] Atanasov M. A., Schmidtke H.-H. (1988) Chem. Phys. **124**: 205
[2] Whangbo M. H., Hoffmann R. (1978) J. Amer. Chem. Soc. **100**: 6093
[3] Matsumoto N., Yamashita M., Kida S. (1978) Bull. Chem. Soc. Jpn. **51**: 2334, 3514
[4] Keller H. J. (1982) Linear Chain Platinum Haloamines. In: Miller J. S. (ed.) Extended Linear Chain Compounds, Vol. 1. Plenum Press, New York, p. 357, and references therein
[5] Craven B. M., Hall D. (1961) Acta Cryst. **14**: 475

[6] Brown K. L., Hall D. (1976) Acta. Cryst. **B32**: 279
[7] Robin M. B., Day P. (1967) Adv. in Inorg. Chem. Radiochem. **10**: 247
[8] Cohen A. J., Davidson N. (1951) J. Amer. Chem. Soc. **73**: 1955
[9] Yamada S., Tsuchida R. (1956) Bull. Chem. Soc. Jpn. **29**: 894
[10] Day P. (1974) Mixed Valence Chemistry and Metal Chain Compounds. In: Keller H. J. (ed.) Low-Dimensional Cooperative Phenomena. Plenum Press, New York, p. 191
[11] Tanaka M., Kurita S., Kojima T., Yamada Y. (1984) Chem. Phys. **91**: 257
[12] Tanaka M., Kurita S., Okada Y., Kojima T., Yamada Y. (1985) Chem. Phys. **96**: 343
[13] Interrante L. V., Browall K. W., Bundy F. P. (1974) Inorg. Chem. **13**: 1158
[14] Tanino H., Kobayashi K. (1983) J. Phys. Soc. Jpn. **52**: 1446
[15] Swihart D. L., Mason W. R. (1970) Inorg. Chem. **9**: 1749
[16] Blanchard W. D., Mason W. R. (1978) Inorg. Chim. Acta **28**: 159
[17] Tuszynski W., Gliemann G. (1979) Z. Naturforsch. **34a**: 211
[18] Vanquickenborne L. G., Ceulemans A. (1981) Inorg. Chem. **20**: 796
[19] Viaene L., Ceulemans A., Vanquickenborne L. G. (1985) Inorg. Chem. **24**: 1713
[20] Whangbo M. H., Foshee M. J. (1981) Inorg. Chem. **20**: 113
[21] Ammeter J. H., Bürgi H. B., Thibeault J. C., Hoffmann R. (1978) J. Amer. Chem. Soc. **100**: 3686
[22] Kroening R. F., Rush R. M., Martin D. S. Jr., Clardy J. C. (1974) Inorg. Chem. **13**: 1366
[23] Williams R. J., Dillin D. R., Milligan W. O. (1973) Acta Cryst. **B29**: 1369
[24] Mais R. H. B., Owston P. G., Wood A. M. (1972) Acta Cryst. **B28**: 393
[25] (a) Larsen K. P., Hazell R. G., Toftlund H., Andersen P. R., Bisgard P., Edlund K., Eliasen M., Herskind C., Laursen T., Pedersen P. M. (1975) Acta Chem. Scand. **A29**: 499; (b) Freckmann B., Tebbe K. F. (1981) Acta Cryst. **B37**: 1520
[26] Viossat P. B., Toffoli P., Khodadad P., Rodier N. (1987) Acta Cryst. **C43**: 855
[27] Clark R. J. H. (1978) Spectroscopic and Structural Studies of Mixed-Valence Linear-Chain Transition-Metal Compounds. In: Ann. NY Acad. Sci., p. 672
[28] Papavassiliou G. C., Rapsomankis R., Mourikis S., Jacobsen C. S. (1982) J. Chem. Soc. Farad. Trans. II **78**: 17
[29] Hitchman M. A. (1982) Inorg. Chem. **21**: 821
[30] Harrison W. A. (1980) Electronic Structure and the Properties of Solids – The Physics of the Chemical Bonds. Freeman, San Francisco, p. 451
[31] Lever A. B. P., Walker I. M., McCarthy P. J., Mertes K. B., Jircitano A., Sheldon R. (1983) Inorg. Chem. **22**: 2252
[32] Jørgensen C. K. (1966) Struct. and Bondg. **1**: 3
[33] Glerup J., Monsted O., Schäffer C. E. (1976) Inorg. Chem. **15**: 1399
[34] Smith D. W. (1978) Struct. and Bondg. **35**: 87
[35] Brust J. (1968) Methods in Computational Physics, Vol. 8. Academic Press, New York, p. 52
[36] Clark R. J. H., Turtle P. C. (1978) Inorg. Chem. **17**: 2526
[37] Interrante L. V., Browall K. W. (1974) Inorg. Chem. **13**: 1162
[38] Shimura Y. (1988) Bull. Chem. Soc. Jpn. **61**: 693

Received March 13, 1989. Accepted March 31, 1989